SUPPORTING ONLINE MATERIAL

Muscle dysfunction caused by a K_{ATP} channel mutation producing neonatal diabetes is neuronal in origin

Rebecca H Clark[1], James S McTaggart[1]*, Richard Webster[2]*, Roope Männikkö[1]*, Michaela Iberl[1], Xiuli Sim[1], Patrik Rorsman[3], Maike Glitsch[1], David Beeson[2], Frances M Ashcroft[1]

[1]*Department of Physiology, Anatomy and Genetics, University of Oxford, Parks Road, Oxford, OX1 3PT, UK*
[2]*Weatherall Institute of Molecular Medicine, University of Oxford, Oxford OX3 9DS, UK*
[3]*Oxford Centre for Diabetes Endocrinology and Metabolism, Churchill Hospital, Oxford OX3 7LJ, UK*

*these authors made equal contributions

MATERIALS AND METHODS

Generation of mutant mice

The Kir6.2-V59M gene, preceded by a loxP-flanked stop sequence and followed by an FRT-flanked IRES GFP cassette, was targeted to the ROSA26 locus to ensure that a single copy of the mutant gene was expressed, from a known location (*S1*). The endogenous ROSA promoter was used to prevent excess gene expression. To generate mice that express the Kir6.2-V59M transgene specifically in muscle, ROSA26StopKir6.2-V59M$^{lox/+}$ mice (ROSA mice) (*S1*) were crossed with mice expressing Cre recombinase under the control of the muscle creatine kinase promoter (Mck-Cre mice). The latter were kindly provided by Prof. Jens Bruning, Institute of Genetics, Cologne. This generated mice (m-V59M mice) in which expression of Cre recombinase in muscle (skeletal and heart) leads to deletion of the stop cassette and thus to expression of the Kir6.2-V59M gene. In a similar fashion, mice expressing the Kir6.2-V59M gene selectively in neurons (n-V59M mice) were generated by crossing ROSA mice with nestin-Cre mice (Jackson Labs). Littermates were used for all studies.

Animal care

All experiments were conducted in accordance with the UK Animals Scientific Procedures Act (1986) and University of Oxford ethical guidelines. Mice were housed in same-sex littermate groups of 2-8, in a temperature and humidity controlled room on a 12h light-dark cycle (lights on at 6 am). Regular chow food (Teklad Global 2019 Rodent (Harlan Teklad, UK) containing 55% carbohydrate, 19% protein and 9% fat) was freely available. Mice had *ad libitum* access to water at all times.

Genotypes were identified by PCR using genomic DNA isolated from ear biopsies, as previously described (*S1*).

Molecular Biology

RNA extraction and cDNA synthesis

Muscle and brain tissues were isolated from m-V59M, n-V59M and control mice, immersed in RNALater solution (Qiagen), kept at 4°C for one hour and thereafter stored at -80°C until ready to process. Total RNA was extracted from 30mg of tissue using an RNeasy Mini Kit (Qiagen), including an on-column DNase digestion step to remove traces of genomic DNA. RNA concentration was determined using a NanoDrop ND-1000 spectrophotometer (Thermo Scientific), and its integrity verified with an Agilent Bioanalyzer. One microgram of total RNA was reverse transcribed in a 20µl final volume using a High Capacity cDNA Reverse Transcription kit (Applied Biosystems). A separate microgram of total RNA was processed identically, but with no reverse transcriptase present (Non-RT control).

Semi-quantitative PCR
Mouse Kir6.2 transcript was amplified by PCR using cDNA prepared from muscle and brain tissues from m-V59M, n-V59M and control mice. Primers used were: forward (5'-ATGCTGTCCCGAAAGGGCAT-3') and reverse (5'-TGGTCTGGTGGCTCATCGCC-3'). After 40 cycles (95°C/30s; 60°C/30s; 72°C/1min), PCR products were digested with BtsCI restriction enzyme (New England Biolabs) for ~2h at 50°C. Digested PCR fragments were visualized on a 2% agarose gel with Ethidium Bromide.

RT-qPCR
All cDNA samples were diluted to 4 ng/µl with nuclease free water (Sigma). Each reaction consisted of 5µl (20ng) cDNA, 12.5µl 2x PowerSYBR Green I Master Mix (Applied Biosystems), 0.75µl 10µM forward and reverse primers (300nM) and 6µl nuclease-free water (total reaction volume 25µl). Reactions were run on an ABI PRISM® 7000 sequence detection system (Applied Biosystems). The reaction cycle comprised an initial denaturation for 10 min at 95°C, followed by 40 cycles of 95°C/15sec; 60°C/60sec. All cDNA samples were run in triplicate. Non-RT controls were included in each experiment to confirm the absence of genomic DNA contamination.

Primers were designed using the Geneious Pro software (Biomatters Ltd) based on NCBI sequence data. Primer specificity was checked using BLAST, gel electrophoresis, and melt curve analysis. Primer efficiencies were calculated using serial dilutions of tissue cDNA and ranged from 1.9 to 2.1 (see Table S3). The geNorm applet for Microsoft Excel was used to determine the most stable genes from a selection of candidate reference genes (*S2*). ACTB, HPRT1 and HSPA8 were identified as being the most stably expressed and were used as reference genes for RT-qPCR. See Table S4 for primer details.

Data analysis and relative expression calculations
The 7000 System SDS Software (Applied Biosystems) was used to acquire and analyse qPCR data and derive cycle threshold (Ct) values. The delta Ct method was used to transform Ct values into relative quantities and the highest expression for each primer pair was set to 1. The geNorm software was used on the three reference genes to calculate normalization factors for each tissue (*S2*). The relative expression levels of Kir6.2 and SUR1 (or SUR2) were calculated using this normalization factor. Differences in gene expression between tissues were analysed using a one-way ANOVA. $P<0.05$ was considered significant. Statistics were performed using SigmaStat (Aspire Software International).

Behavioural phenotyping
Mice were tested for muscle strength and motor coordination at 11-12 weeks of age. Testing was carried out over a maximum period of 48 hours. We found no difference between male and female mice, so the data were pooled. All behavioural experiments were performed blinded with respect to the genotype of the animal.

Three tests of muscle strength were used: weight lifting, inverted screen, and horizontal bar, as detailed elsewhere (*S3*). Briefly, the first test allows a quantification of strength.

The mouse was allowed to grasp a series of increasingly heavy weights that consisted of between 1-5 links cut from a light chain. It was then picked up by its tail. The score was calculated as the number of chain links held for 3s multiplied by the time for which it was held. For the inverted screen test, mice were placed in the centre of a wire grid, which was then inverted and held 30cm above a soft surface. The time at which the mouse fell was scored 1 (110s or less before falling), 2 (110-250s), 3 (251-599s) or 4 (600s or more). Little coordination is needed to grip the screen with all four feet so this test measures muscle strength. The horizontal bar test measures both the strength of the forelimbs and motor coordination. It comprised a 38cm-long, 2mm-thick brass bar held 49cm above a padded bench surface by supporting columns at each end. The mouse was placed at the centre of the bar hanging from its forepaws. It was left holding the bar for a maximum of 30s or removed if it reached an end column. Each of these was awarded the maximum score of 5. Falls at earlier times received a graded score: 1 (5s or less on the bar), 2 (6-10s), 3 (11-20s) to 4 (21-29s).

The static rod test was used to measure motor coordination. A static wooden rod, 600mm long and 9mm in diameter was fixed at one end above a drop of 40cm. Padding was provided to cushion any falls. Each mouse was placed 20mm away from the protruding end, facing away from the bench. The time to turn around 180° (while remaining upright) and whether or not the mouse fell off before it reached the end of the rod was measured.

The rotarod measures coordination on a rod rotating about its long axis. An accelerating rotarod (Ugo Basile, Italy, model 7650) was modified to have a start speed of 2.5 r.p.m. and an acceleration rate of 20 r.p.m./min. A mouse was placed on the rod, which was accelerated after 10s. The time from the start of acceleration until when the mouse fell was noted, up to a maximum time of 120s.

Spontaneous locomotor activity was measured in two ways. First, mice were kept for 23hr in a cage containing a running wheel: the duration of the time they spent on the free-running wheel, the speed of running, and the distance travelled were measured. Second, their activity was monitored over 23hr using a Home Cage Threshold Activity System monitor (Med Associates, St Albans VT).

Statistics
When the data distribution permitted (i.e. fulfilled the criteria of normality and equality of variance), a one-way ANOVA was performed. Data obtained using the inverted screen, horizontal bar and weight-lifting tests were analysed using a non-parametric test, the Kruskal-Wallis One Way Analysis of Variance on Ranks. $p<0.05$ was considered statistically significant.

Electrophysiology

Neuromuscular junction
For the phrenic nerve/hemidiaphragm preparation, mice were killed by exposure to a raised CO_2 atmosphere followed by cervical dislocation. Phrenic nerve/hemidiaphragm

preparations were dissected from the mouse thorax and bathed in Krebs solution, bubbled with 95%O_2/5%CO_2. Preparations were pinned out in a Sylgard-coated Petri dish containing bubbled Krebs solution (in mM): NaCl 118, KCl 4.7, $MgSO_4$ 1.2, KH_2PO_4 1.2, $NaHCO_3$ 24.9, Glucose 10, $CaCl_2$ 2.5.

The phrenic nerve was stimulated via a suction electrode coupled to a pulse generator (GRASS instruments S48, solid-state square wave stimulator, Quincy, U.S.A.) with an associated stimulus isolation unit. To enable measurement of evoked potentials, the muscle action potential and contraction was blocked with 2.5μM μ-conotoxin GIIIB (Peptide Institute, Japan). Neuromuscular transmission viability was checked before contractile blockade. Recordings were made in Krebs solution at room temperature (20-22°C) using an Axoclamp-2A amplifier (Axon Instruments, Molecular Devices, USA).

Nerve evoked endplate potentials (EPPs) and spontaneous miniature endplate potentials (MEPPs) were recorded intracellularly with conventional borosilicate glass electrodes filled with 3M KCl (10-15MΩ resistance; Harvard Apparatus, Edenbridge, Kent UK) and filtered at 1kHz. Electrodes were positioned above endplate regions, as visualised with a stereomicroscope, under micromanipulator control. Impalement adjacent to an endplate was indicated by a fast EPP rise time (less than 2ms). To evoke an EPP the nerve was stimulated supramaximally with platinum wire electrodes. Upon impalement, a 30s period of equilibration was allowed before MEPP recordings began. If the membrane potential drifted by more than 5mV or depolarised positive to -55mV the recording from that endplate was abandoned. Data signals were passed through a "Humbug 50 Hz noise eliminator" (Quest Scientific via Digitimer, Welwyn Garden City, UK) to reduce electrical noise on recordings. 20-30 EPPs (stimulated at 1 Hz) were recorded per endplate. Recordings from many endplates were accumulated over a 90min period. Up to 30 MEPPs were recorded per endplate for later offline analysis. Recorded MEPPs and EPPs were digitised at 10 kHz (Axon Digidata 1322A interface, Molecular Devices, USA). Each MEPP and EPP was detected via template searching in pClamp 9 software. MEPP and EPP amplitude measurements were not adjusted for differences in resting membrane potential. Mean quantal content (*m*) was calculated using the membrane potential corrected MEPP and EPP amplitude, using the direct method using the formula:

$$m = \text{mean}(AMP_{EPP})/\text{mean}(AMP_{MEPP}) \qquad \text{eqn.1}$$

where AMP_{EPP} is the corrected amplitude of the EPP and AMP_{MEPP} is the amplitude of the MEPP. Mean EPPs were corrected for non-linear summation using the formula (*S4*).

$$AMP_{EPP} = AMP_{EPP\ (measured)}/[(1-0.8\ AMP_{EPP\ (measured)}) / E] \qquad \text{eqn.2}$$

where E is the adjusted resting membrane potential (-80 mV) and 0.8 is the correction factor for mouse endplates.

K_{ATP} channel recordings from mouse muscle fibres

Mice were killed by cervical dislocation. The flexor digitalis brevis (FDB) muscles of the

hind limb were isolated and exposed to 2.5 mg/ml Liberase TL (Roche Applied Science, Mannheim, Germany) dissolved in Ringer (in mM: 150 NaCl, 5 KCl, 2 $MgCl_2$, 1 $CaCl_2$, 10 HEPES, pH 7.4) for 30-60 min at 37ºC on a shaking table. The muscles were thoroughly rinsed with Ca^{2+}-free Ringer (in mM: 150 NaCl, 5 KCl, 1 $MgCl_2$, 0.5 EGTA, 10 HEPES, pH 7.4). Single muscle fibres were dissociated in flowing Ca^{2+}-free Ringer solution. Fibres were allowed to settle on the bottom of a Petri dish for >15 min during which time blebs formed spontaneously on the fibre surface. K_{ATP} channel activity was recorded in patches excised from these blebs. The pipette solution contained (in mM): 140 KCl, 1.2 $MgCl_2$, 2.6 $CaCl_2$, 10 HEPES, pH 7.4). The intracellular solution contained (in mM): 155 KCl, 11 EGTA, 2 $MgCl_2$, 1 $CaCl_2$, 10 HEPES, pH 7.2) with MgATP as indicated.

Xenopus oocytes

Human Kir6.2 (Genbank NM000525; E23 and I337), rat SUR1 (Genbank L40624) and rat SUR2A (Genbank83598) were used in this study. Site-directed mutagenesis, synthesis of capped mRNA and preparation of *Xenopus laevis* oocytes were performed as previously reported (*S5)*. Oocytes were coinjected with ~4ng of SUR1 or SUR2A mRNA and ~0.8ng of wild-type or mutant Kir6.2 mRNA. To simulate the heterozygous state, SUR1 (or SUR2A) was coexpressed with a 1:1 mixture of wild type and mutant Kir6.2. Oocytes were incubated in Barth's solution supplemented with 50 μg/ml tetracycline and 50 μg/ml gentamycin and studied 1-4 days after injection.

Whole-cell currents were recorded using a two-electrode voltage-clamp in response to voltage steps of ±20mV from a holding potential of –10mV, in a solution containing (in mM): 90 KCl, 1 $MgCl_2$, 1.8 $CaCl_2$, 5 HEPES (pH 7.4 with KOH). Metabolic inhibition was induced by 3mM Na-azide. Diazoxide (300μM) was used to activate and tolbutamide (0.5mM) to block SUR1-K_{ATP} channels. Pinacidil (100μM) was used to activate and glibenclamide (10 μM) to block SUR2A-K_{ATP} channels.

ATP concentration-response relationships were measured in giant inside-out patches. The pipette solution contained (mM): 140 KCl, 1.2 $MgCl_2$, 2.6 $CaCl_2$, 10 HEPES (pH 7.4 with KOH). The intracellular solution contained (mM): 107 KCl, 11 EGTA, 2 $MgCl_2$, 1 $CaCl_2$, 10 HEPES (pH 7.2 with KOH) plus adenosine nucleotides as indicated. Conductance at -60mV (G) was expressed as a fraction of that in ATP-free solution (Gc). To control for possible rundown or activation by MgATP, G_C was taken as the mean of the conductance in control solution before and after ATP application. ATP concentration-response curves were fit with a modified Hill equation:

$$G/G_C = a + (1 - a) / (1 + ([ATP] / IC_{50})^h), \qquad \text{eqn 3}$$

where [ATP] is the ATP concentration, IC_{50} is the ATP concentration at which inhibition is half maximal, *h* is the slope factor (Hill coefficient) and *a* represents the fraction of unblocked current at saturating [ATP] (a=0 except where specified).

All K_{ATP} channels show a decline in channel activity following patch excision, a

phenomenon known as 'rundown'. The rate and extent of rundown varied between patches and channel type. This complicates quantitation of the extent of MgADP activation, which can appear greater for channels that are more rundown if activation is expressed as the increase in current between that in MgADP solution and in the adjacent control solution. To normalize for differing extents of rundown, therefore, we expressed the K_{ATP} current in the presence of MgADP as a fraction of the maximal current following patch excision.

Brain Slices

Sagittal brain slices (200µm) containing the vermis were prepared from 2- to 3-week old male and female control and n-V59M mice. They were allowed to recover for at least 45 mins at 20-23°C in aCSF solution containing (in mM): 125 NaCl, 21 $NaHCO_3$, 2.5 KCl, 1.2 NaH_2PO_4, 10 HEPES (pH7.4 with NaOH), 2 $CaCl_2$, 2 $MgCl_2$, 5 glucose, gassed with 95% O_2 and 5% CO_2. Brain slices were then transferred to a recording chamber and continuously perfused at 2–4 ml/min with gassed aCSF. Tolbutamide (200µM or 500µM) was added as indicated. For whole-cell recordings, patch pipettes were filled with internal solution containing (in mM) 128 K-gluconate, 10 KCl, 10 HEPES, 1 EGTA, 2 $MgCl_2$, 0.3 Na-GTP, and 3 K_2-ATP, pH 7.3 adjusted with KOH. For cell-attached recordings, pipettes were filled with aCSF solution. Experiments were carried out at 20-23°C. Whole-cell recordings were acquired using an EPC-9 patch-clamp amplifier (HEKA). Data were filtered, sampled with Pulse/Pulsefit software (Heka Electronik) and analyzed with Pulsefit 8.67 and Sigmaplot.

The membrane potential of firing neurons was determined from slow time-scale recordings on which a clear basal line was evident; this baseline was taken as the resting potential (*S7)*. Firing frequency was calculated using Pulsefit software. For whole-cell recordings, firing rate was calculated for durations of 1 minute, ~5min after breaking into the cell (basal) or 5min after addition of tolbutamide, at which times the firing rate had stabilised. For cell-attached recordings, firing was measured as the average rate during three 10s sections spaced one minute apart. We found no differences between different types of control mice, so the data were pooled.

SUPPORTING TEXT

Figure 1A

The relative extent of wild-type (WT) and mutant Kir6.2 mRNA expression was estimated by exploiting the fact that introduction of the V59M mutation removes a unique BtsCI restriction site. Kir6.2 transcripts amplified by RT-PCR from tissue isolated from control, m-V59M or n-V59M mice were digested with BtsCI and loaded on a 2% agarose gel. Amplification of WT Kir6.2 cDNA generates a 282bp product, which is cleaved by BtsCI into 177bp and 105bp products (arrowed). Introduction of the V59M mutation removes the unique BtsCI restriction site, preventing cleavage. Thus two bands indicate the presence of the wild-type gene only and three bands indicates both wild-type and mutant genes. The relative amount of expression can be estimated by the relative intensities of the two bands. The similar intensities seen for all three bands in tissues in which Kir6.2-V59M is selectively expressed suggests the mutant gene is expressed at roughly similar levels to wild-type. This is confirmed by the fact that the IC_{50} for ATP inhibition of K_{ATP} channels in skeletal muscle of m-V59M mice (67±11μM) is not significantly different from that found for hetKir6.2-V59M/SUR2A channels heterologously expressed in *Xenopus* oocytes (79±18μM, Table S2). This indicates that the mouse provides a plausible model for the heterozygous state of patients carrying the Kir6.2-V59M mutation.

Figure 4

(**B**) The smooth curves are best fit of the mean data with the Hill equation (eqn 3) with the following parameters: Kir6.2/SUR1 (IC_{50}=13μM, h=1.0), Kir6.2/SUR2A (IC_{50}=18μM, h=0.9), hetKir6.2-V59M/SUR1 (IC_{50}=38μM, h=0.93, a=0.06), hetKir6.2/SUR2A (IC_{50}=57μM, h=0.807, a=0.02). Mean values, obtained by fitting each concentration-response curve individually, are given in Table S1.

(**D,E**) The smooth curves are best fit of the mean data with the Hill equation (eqn 3) with the following parameters. (**D**), HetKir6.2-V59M/SUR1 in the absence (IC_{50}=38μM, h=0.93, a=0.06) and the presence (IC_{50}=184μM, h=1.03, a=0.05) of 100μM MgADP. (**E**), HetKir6.2-V59M/SUR2A in the absence (IC_{50}=57μM, h=0.80, a=0.02) and the presence (IC_{50}=64μM, h=1.04, a=0.02) of 100μM MgADP. Mean values obtained by fitting each concentration-response curve individually are given in Table S2.

SUPPORTING FIGURES

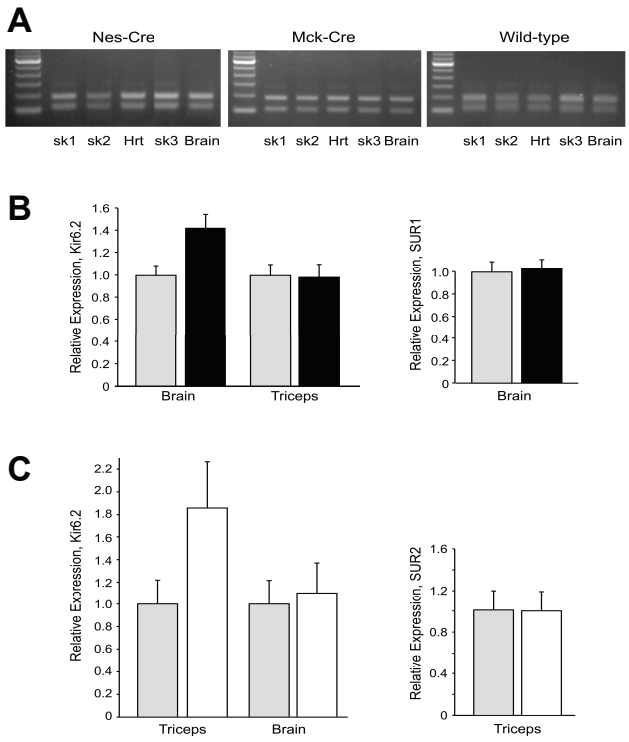

Figure S1

(**A**) Kir6.2 expression in tissue isolated from a Nes-Cre, Mck-Cre or wild-type mouse. Wild-type (WT), but not mutant, cDNA is cut by the restriction enzyme BtsCI: the presence of two bands thus indicates the presence of the wild-type gene only and three bands indicates both wild-type and mutant genes. sk1, quadriceps muscle; sk2, triceps muscle; sk3, diaphragm; Hrt, heart. Data are representative of experiments on 4 WT, 4 Nes-Cre and 4 Mck-Cre mice. Experiments were also done in parallel on 4 m-V59M mice, 3 n-V59M mice and 7 ROSA mice (Fig.1A).

(**B**) Quantitative PCR showing expression of Kir6.2 in brain and muscle (*left*) and SUR1 in brain (*right*) of control mice (grey bars, n=6) and n-V59M mice (black bars, n=6), relative to levels of a panel of house-keeping genes (see Methods). SUR1 mRNA levels were unchanged in brain of n-V59M mice. Kir6.2 levels were increased about ~40%. However, channel density should remain relatively constant as SUR1 is unchanged and both subunits are needed to form a functional channel. There was no change in Kir6.2 expression in muscle of n-V59M mice (One-way ANOVA). Data are mean ± SEM.

(**C**) Quantitative PCR showing expression of Kir6.2 in muscle and brain (*left*) and SUR2 in muscle (*right*) of control (grey bars, n=5) and m-V59M mice (white bars, n=5), relative to a panel of house-keeping genes. Kir6.2 levels were increased about ~80% in muscle of m-V59M mice. However, channel density should remain relatively constant as SUR2 mRNA was unchanged. There was also no change in Kir6.2 expression in brain of m-V59M mice (One-way ANOVA). Data are mean ± SEM.

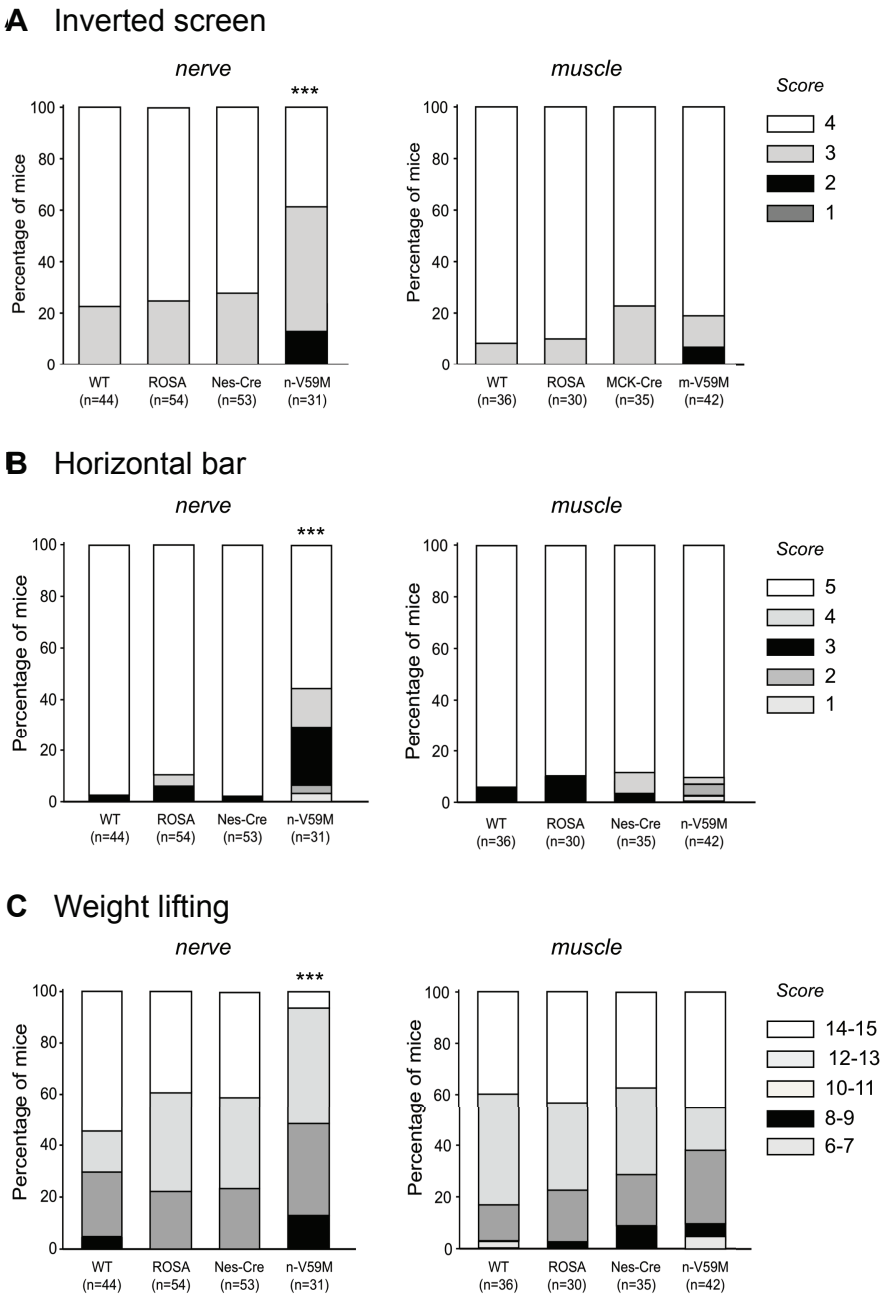

Figure S2

(**A**) inverted screen, (**B**) horizontal bar and (**C**) weight-lifting tests carried out on 12-week old wild-type (WT, n=44), ROSA (n=54), Nes-Cre (n=53) and n-V59M (n=31) mice (*left*); and on 11-week old WT (n=36), ROSA (n=30), Mck-Cre (n=35) and m-V59M (n=42) mice (*right*). The percentage of mice achieving the indicated score is shown. ***, $p<0.001$ against Nes-Cre, WT and ROSA controls (Kruskal-Wallis One Way Analysis of Variance on Ranks).

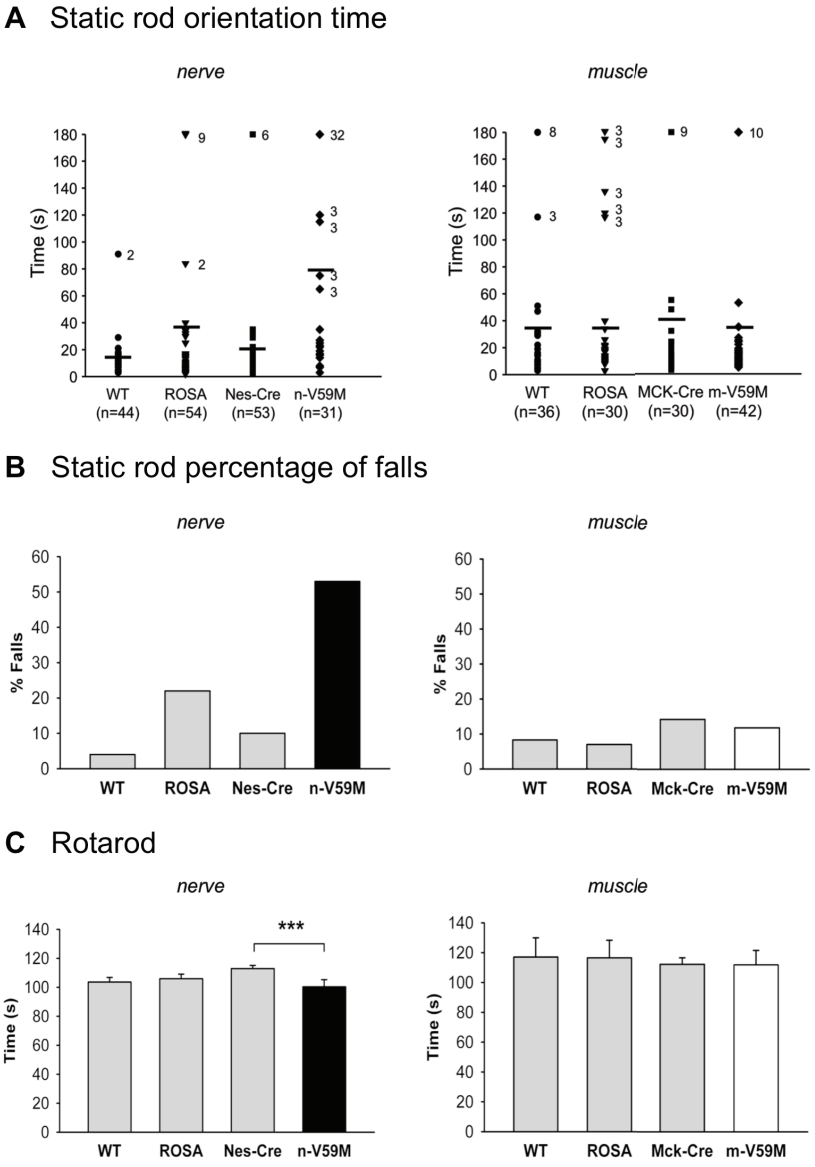

Figure S3

Motor coordination tests carried out on 12-week old wild-type (WT, n=44), ROSA (n=54), Nes-Cre (n=53) and n-V59M (n=31) mice (*left*); and on 11-week old WT (n=36), ROSA (n=30), Mck-Cre (n=35) and m-V59M (n=42) mice (*right*). (**A**) Orientation time on a static rod. All data points are indicated and the numbers adjacent to the data points indicate the percentage of mice achieving that time. The horizontal line indicates the median. Mck-Cre and m-V59M mice may take longer than Nes-Cre mice to orient on the static rod because they weigh more (Fig. S8). (**B**), Percentage of falls off the static rod. (**C**) Time before falling off a rotating rod. Data are mean ± SEM. *** $p<0.001$ (One-way ANOVA).

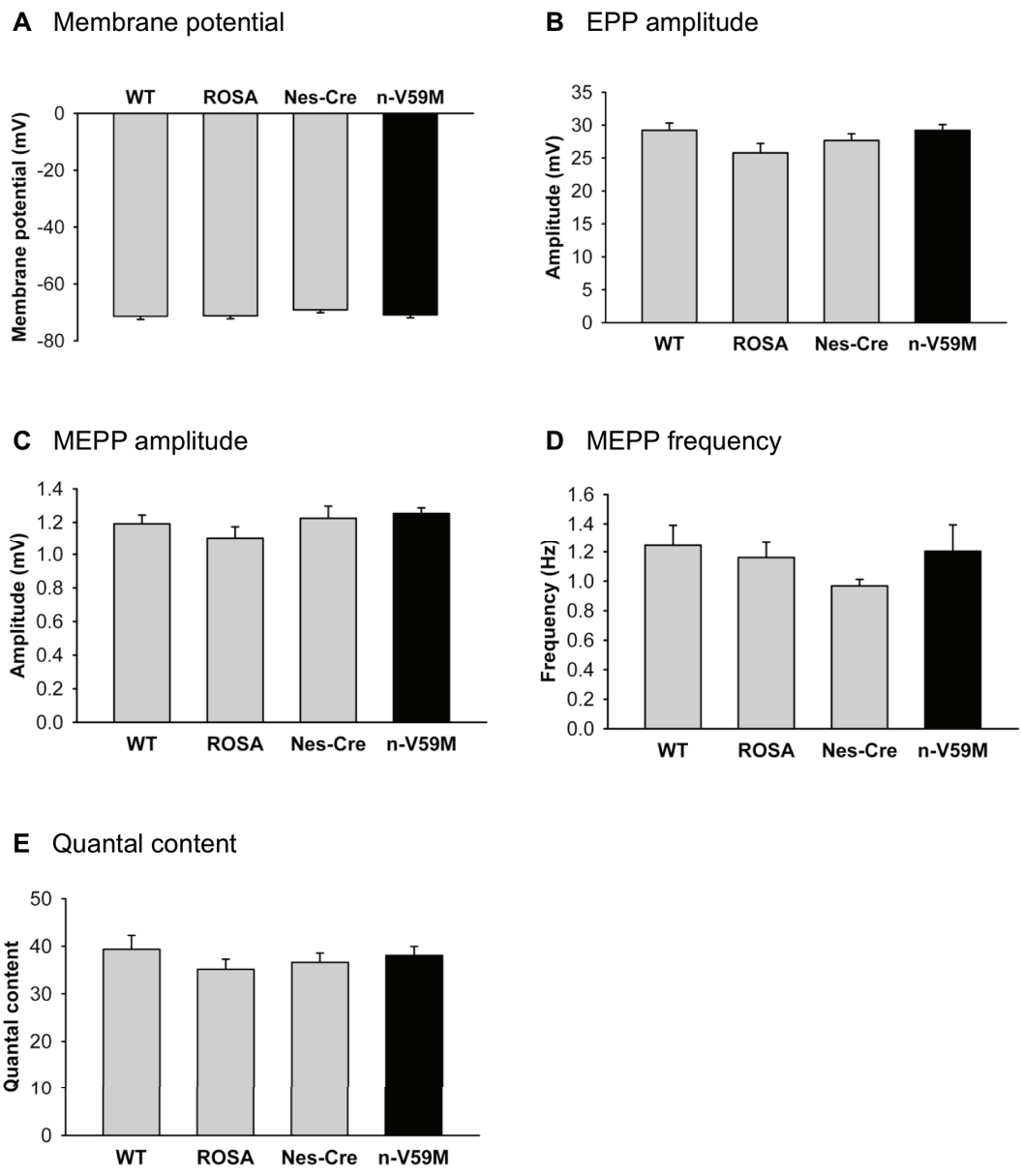

Figure S4
Mean membrane potential (**A**), endplate potential (EPP) amplitude (**B**), miniature endplate potential (MEPP) amplitude (**C**) and frequency (**D**), and quantal content (**E**) measured in phrenic nerve/hemidiaphragm muscle preparations isolated from 12-week old wild-type (WT, n=8), ROSA (n=8), Nes-Cre (n=7) and n-V59M (n=8) mice. Data are mean ± SEM.

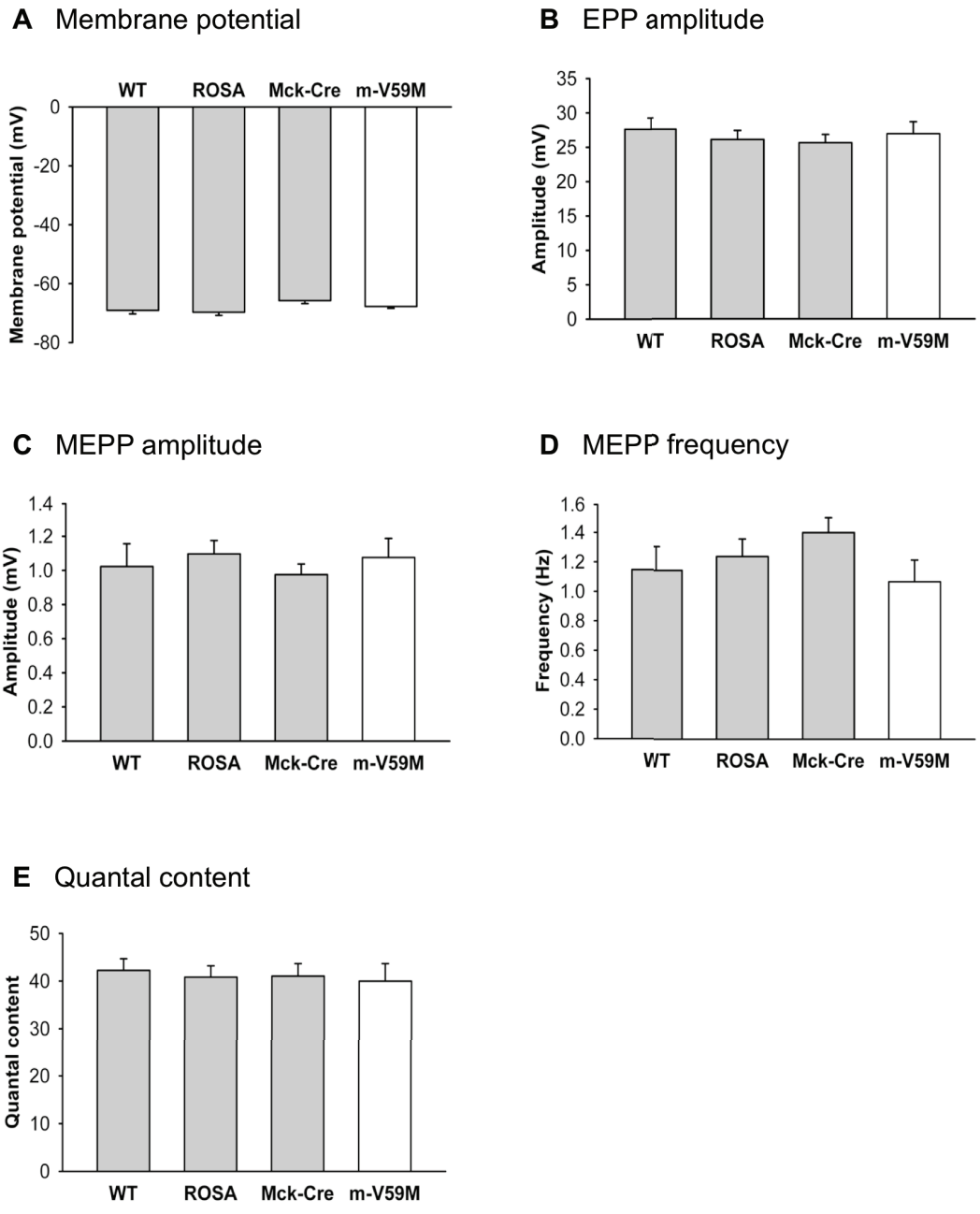

Figure S5
Mean membrane potential (**A**), end-plate potential (EPP) amplitude (**B**), miniature end-plate potential (MEPP) amplitude (**C**) and frequency (**D**), and quantal content (**E**) measured in the phrenic nerve/hemidiaphragm muscle preparation isolated from 12-week old wild-type (WT, n=8), ROSA (n=8), Mck-Cre (n=5) and mV59M (n=5) mice. Data are mean ± SEM.

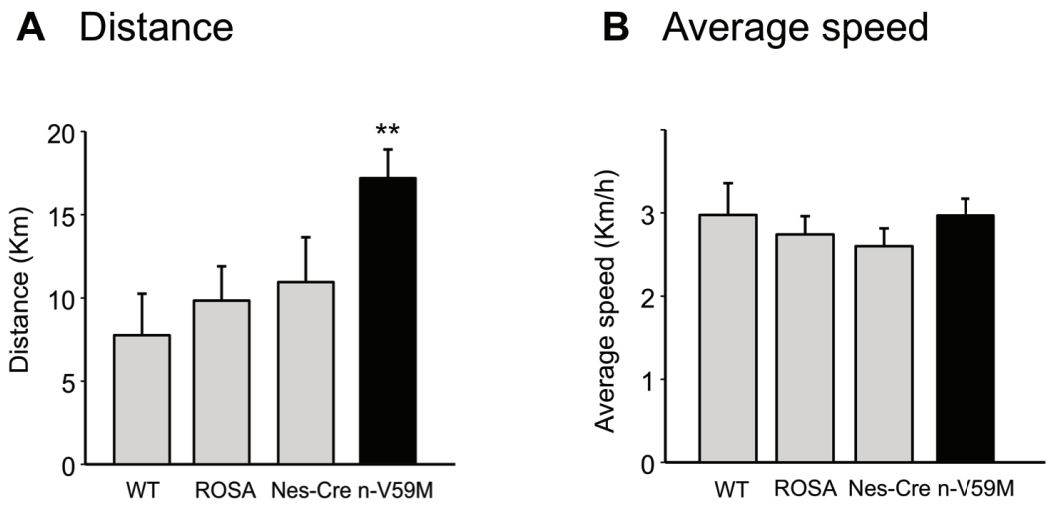

Figure S6
Distance ran (**A**), and average speed (**B**) over a 23-hour period on a free-running wheel for 12-week old wild-type (WT, n=4), ROSA (n=14), Nes-Cre (n=14), and n-V59M (n=13) littermates. Data are mean ± SEM. ** $p<0.01$ (One-way ANOVA).

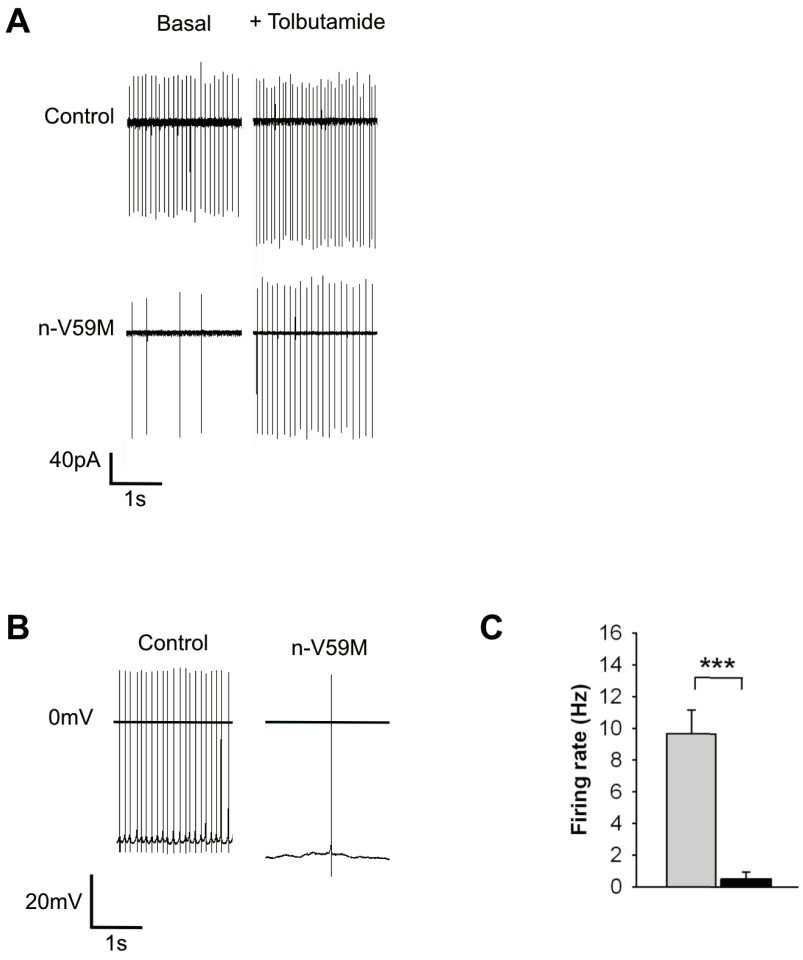

Figure S7

(**A**) Representative cell-attached recordings from cerebellar Purkinje neurons of control (*above*) or n-V59M (*below*) mice in the absence (*left*) and presence (*right*) of 500µM tolbutamide.

(**B**) Representative whole-cell current clamp recording of electrical activity in Purkinje neurons of control (*left*) and n-V59M (*right*) mice. The horizontal lines indicate 0mV.

(**C**) Mean action potential frequency of control Purkinje neurons (grey bar, n=6 mice, 17 cells) and n-V59M Purkinje neurons (black bar, n=5 mice, 13 cells). Current clamp recordings in the whole-cell configuration. Data are mean ± SEM. ***, $p<0.001$.

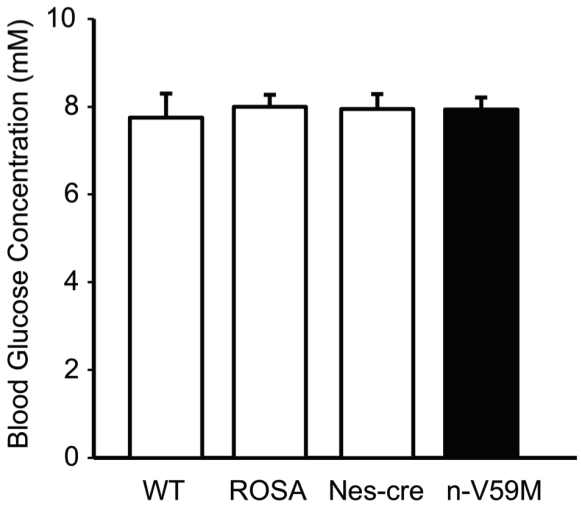

Figure S8
Free-fed blood glucose levels of wild-type (WT, n=3), ROSA (n=6), Nes-Cre (n=6) and n-V59M (n=8) mice. Blood glucose was measured daily at 3pm, with an Analox blood glucose monitor. We show a representative example for one day measured for *n* mice. Data are mean ± SEM.

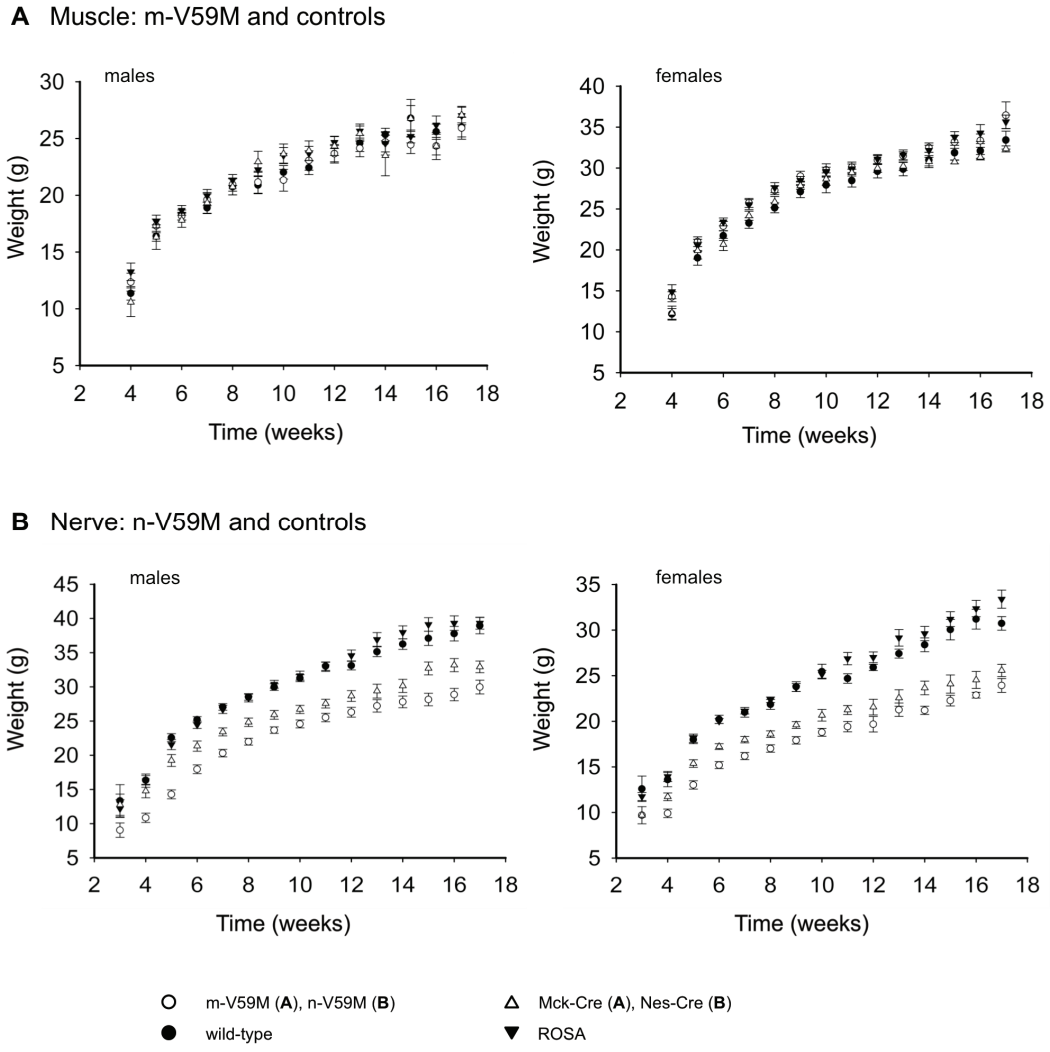

Figure S9

(**A**) Mean body weights of male and female m-V59M mice and wild-type (WT), ROSA and Mck-Cre littermates. n=14-30 mice of each type. (**B**) Mean body weights of male and female n-V59M mice and WT, ROSA and Nes-Cre littermates. n=14-27 mice of each type. Open circles, m-V59M (**A**, muscle) or n-V59M (**B**, nerve). Open triangles, Mck-Cre (**A**, muscle) or Nes-Cre (**B**, nerve). Filled circles, WT. Filled triangles, ROSA. Nes-Cre and n-V59M mice had lower body weights than WT or ROSA mice. However there was no significant difference between the weights of Nes-Cre and n-V59M mice. Data are mean ± SEM.

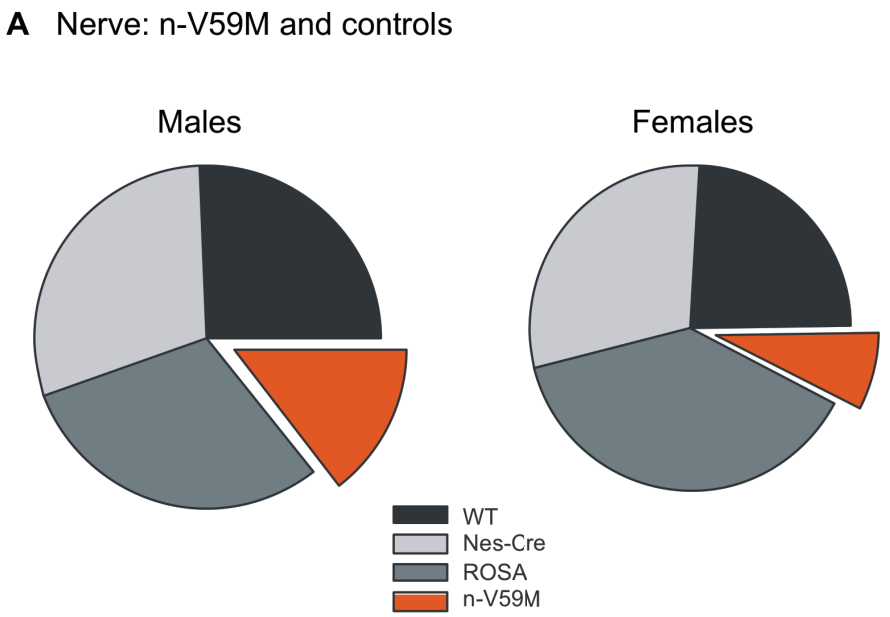

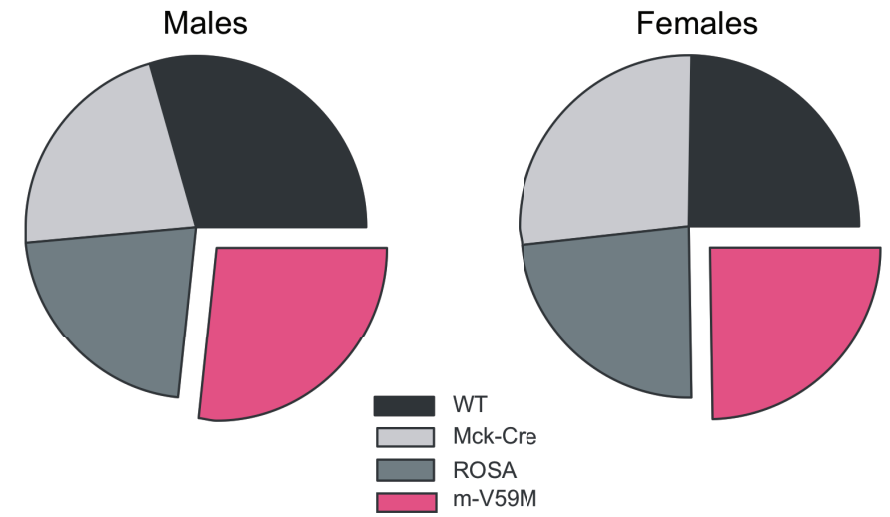

Figure S10
(**A**) Birth frequency of male (*left*) and female (*right*) wild-type (WT, n=62), ROSA (n=83), Nes-Cre (n=74) and n-V59M (n=29) mice. n-V59M mice (especially females) were born at less than Mendelian frequency.
(**B**) Birth frequency of male (*left*) and female (*right*) WT (n=52), ROSA (n=43), Mck-Cre (n=46) and m-V59M (n=49) mice.

SUPPORTING TABLES

TABLE S1

ATP concentration-inhibition curves for K_{ATP} channels were measured in inside-out patches excised from control and m-V59M FDB muscle (i.e. native Kir6.2/SUR2A and Kir6.2-V59M/SUR2A channels). The data are the mean ± SEM of the fits of the individual ATP concentration-inhibition curves with eqn 3. ** $p<0.01$ against control (Student's t-test). Note that the IC_{50} for m-V59M mice (67µM) is not significantly different from that found for hetKir6.2-V59M/SUR2A channels expressed in *Xenopus* oocytes (79µM, Table S2). This indicates that the mouse recapitulates the heterozygous state of the patients, as also demonstrated in Fig.1 of the main text and Fig. S1.

	IC_{50} (µM)	*h*	*a*	n
control	17 ± 3	1.3 ± 0.2	-	4
m-V59M	67 ± 11**	1.4 + 0.2	0.02 ± 0.02	4

TABLE S2

ATP concentration-inhibition curves for Kir6.2/SUR and Kir6.2-V59M/SUR channels expressed in *Xenopus* oocytes, in the presence and absence of 100µM MgADP. The data are the mean ± SEM of the fits of the individual ATP concentration-inhibition curves with eqn 3. * $p<0.05$, ** $p<0.01$, ***$p<0.001$ against WT (Student's t-test). Data in the presence of 100µM MgADP are significantly different from that in the absence of MgADP for Kir6.2/SUR1 ($p<0.001$) and Kir6.2-hetV59M/SUR1 ($p<0.001$) channels but not for Kir6.2/SUR2A ($p=0.22$) or Kir6.2-hetV59M/SUR2A ($p=0.74$) channels. (Student's t-test).

Kir6.2	SUR	0 ADP		100µM MgADP	
		IC_{50} (µM)	n	IC_{50} (µM)	n
WT	SUR1	14 ± 1	15	51 ± 8	5
hetV59M	SUR1	45 ± 7***	12	213 ± 29**	14
WT	SUR2A	22 ± 3	15	29 ± 4	12
hetV59M	SUR2A	79 ± 18**	16	70 ± 11***	7

TABLE S3

Primer sequences and efficiencies for RT-qPCR. Primers were designed with the Geneious Pro software (Biomatters Ltd) based on NCBI sequence data. Their specificity was verified via BLAST, gel electrophoresis and melt-curve analysis. Primer efficiencies were calculated using serial dilutions of tissue cDNA.

Short Name	Primer	Sequence (5' to 3')	Amplicon size (bp)	Efficiency
ACTB	fwd	GCAGCTCCTTCGTTGCCGGT	132	2.1
	rev	TACAGCCCGGGGAGCATCGT		
HPRT1	fwd	CCGGCAGCGTTTCTGAGCCA	123	2.1
	rev	GCTCGCGGCAAAAAGCGGTC		
HSPA8	fwd	CAGCGCAGCTGGGCCTACAC	152	1.9
	rev	TAGCTTGGCGTGGTGCGGTT		
GFP	fwd	CGGCGACGTAAACGGCCACA	103	2.1
	rev	CAGCTTGCCGGTGGTGCAGA		
SUR1	fwd	ACAGCCTTCGCAGACCGCAC	106	1.9
	rev	GCCCGAGCCAGGCAGAACAG		
SUR2	fwd	GCAATCAAAACCAATAAACAGG	132	1.9
	rev	CCCCATGAGAAGTATCCATT		
Kir6.2	fwd	CGGGCGCATGGTGACAGAGG	126	2.0
	rev	CGATGGGCCTGGGCCGTTTT		

TABLE S4

Primer names and details for RT-qPCR. Accession numbers refer to the NCBI database.

Short Name	Full Name	Accession number
ACTB	Beta Actin	NM_007393
HPRT1	Hypoxanthine Guanine Phophoribosyl Transferase 1	NM_013556
HSPA8	Heat Shock Protein 8	NM_031165
GFP	Green fluorescent protein	
SUR1	ATP-binding cassette, sub-family C (CFTR/MRP), member 8	NM_011510
SUR2	ATP-binding cassette, sub-family C (CFTR/MRP), member 9	NM_005691
Kir6.2	Potassium inwardly rectifying channel, subfamily J, member 11	NM_010602

SUPPORTING REFERENCES

S1. C.A. Girard *et al., J. Clin. Invest.* **119**, 80-90 (2009).
S2. J. Vandesompele *et al., Genome Biology.* **3**, research0034.1-0034.11 (2002).
S3. R.M. Deacon *et al., Physiol. Behav.* **87**, 723-733 (2006).
S4. E.M. McLachlan and A.R. Martin, *J. Physiol*. **311**, 307-324 (1981).
S5. P. Tammaro, P. Proks, F.M. Ashcroft, *J. Physiol*. **571**, 3-14 (2006).
S6. L. Plum, *et al.*, *J. Clin. Invest.* **116**,1886–1901 (2006).